CHEMDFM-R: A CHEMICAL REASONING LLM ENHANCED WITH ATOMIZED CHEMICAL KNOWLEDGE

Anonymous authors
Paper under double-blind review

ABSTRACT

While large language models (LLMs) have achieved impressive progress, their application in scientific domains such as chemistry remains hindered by shallow domain understanding and limited reasoning capabilities. In this work, we focus on the specific field of chemistry and develop a Chemical Reasoning LLM, **ChemDFM-R**[1]. We first construct a comprehensive dataset of atomized chemical knowledge, *ChemFG*, annotating the presence of functional groups in molecules and the changes of functional groups during chemical reactions, to enhance the model's understanding of the fundamental principles and internal logic of chemistry. Then, we propose a *mix-sourced distillation* method that integrates expertise in atomized knowledge with general reasoning skills, followed by domain-specific reinforcement learning to enhance chemical reasoning. Experiments on diverse chemical benchmarks demonstrate that ChemDFM-R achieves cutting-edge performance while providing interpretable, rationale-driven outputs. Further case studies illustrate how explicit reasoning chains significantly improve the model's reliability, transparency, and practicality in real-world human-AI collaboration scenarios.

1 INTRODUCTION

With the remarkable capabilities and performance demonstrated by large language models (LLMs) (Brown et al., 2020; Achiam et al., 2023; Team et al., 2023), the development of domain-specialized LLMs has emerged as a popular approach to addressing complex problems (Hendrycks et al., 2020; Chen et al., 2021; Wang et al., 2024). Specifically, in the scientific domain, many efforts focus on either specializing LLMs for specific tasks (Yu et al., 2024; Antunes et al., 2024; Sriram et al., 2024) or building general-purpose scientific assistants (Zhao et al., 2025b; Zhang et al., 2024a; Zhao et al., 2024; Zhang et al., 2025b; Tan et al., 2025). However, given the inherent complexity and high demand for reliability in the scientific domain, current models often struggle with inadequate performance and limited interpretability, which significantly hinders their practicality.

Recently, great success has been achieved in constructing reasoning LLMs in the general domain (Jaech et al., 2024; Guo et al., 2025; Team et al., 2025; Comanici et al., 2025). Beyond enhancing overall model performance, the reasoning-before-answering pattern directly demonstrates how and why the LLM arrives at the answer, thereby markedly improving the reliability and interpretability of the LLM's response. Through the generated rationale, people can confirm the correctness of the answer or identify why the model makes mistakes. Therefore, reasoning-augmented LLMs offer a new promising approach to addressing the aforementioned challenges in scientific-domain LLMs, potentially enhancing their practical utility.

Currently, the research on reasoning LLMs has predominantly focused on general domains, such as mathematics (Yang et al., 2024b; Shao et al., 2024) and programming (Zhu et al., 2024; Hui et al., 2024). In contrast, the reasoning capability of existing LLMs remains highly limited in scientific domains. There are two reasons that hinder current LLMs from excelling in scientific-domain reasoning. 1) The understanding of domain knowledge remains superficial owing to the shortage of in-depth enough training data. The advanced domain knowledge is typically insufficient in general-purpose corpora, while even in current domain-specific corpora, the domain knowledge is still shallow. Current domain-specific corpora (Taylor et al., 2022; Xie et al., 2023; Zhao et al.,

[1]The inference code and the model parameters will be open-sourced.

2025b; Zhang et al., 2024a; Yu et al., 2024) often focus on literature text and high-level phenomena and fail to conduct a proper breakdown into internal mechanisms and atomized knowledge points. For example, in the field of chemistry, the types and positions of *functional groups* within molecules fundamentally determine molecules' properties and reactivities. However, instead of training on functional-group-level knowledge, current chemical LLMs usually directly learn molecule-level knowledge about properties and reactivities. The lack of atomized knowledge significantly constrains the capacity of these models for providing high-quality rationales. 2) The intrinsic reasoning logic in these domains differs significantly from that in mathematics and programming, making it difficult for models to generalize relevant reasoning skills through training in general domains. This not only prevents general-domain LLMs from performing high-quality reasoning in scientific domains, but also introduces additional challenges for building domain-specific reasoning models, which usually involve distillation before reinforcement learning. The common distillation method involves gathering rationales from advanced reasoning LLMs, such as DeepSeek-R1 (Guo et al., 2025) and o3-mini (OpenAI, 2025b), and training student models using supervised finetuning. This process assumes that the teacher LLM is capable of generating sufficiently reasonable rationales. However, this assumption often fails to hold in the scientific fields, such as the chemical domain. Owing to the limited understanding of atomized knowledge and chemical logic, even powerful general-domain reasoning models will highly probably fail to generate accurate and in-depth reasoning for chemical problems.

In this work, we focus on addressing the two aforementioned challenges in the chemistry domain and develop a chemical reasoning LLM, ChemDFM-R. Specifically, we consider the presence of functional groups in molecules and the changes of functional groups during reactions to be atomized knowledge points. We develop a toolkit to identify these features from molecules and reactions and incorporate them into the domain pretraining corpus. The resulting corpus contains over 101 billion tokens from 12 million literature, 30 million molecules, and 7 million reactions. To equip the model with the capability of chemistry-specific reasoning, we develop a mix-sourced distillation process that can take advantage of both the expertise in the carefully curated knowledge points and the advanced reasoning capabilities of general LLMs. Domain-specific reinforcement learning is applied after the distillation process to integrate different capabilities the model learned from corresponding sources and further enhance the reasoning capability. The resulting model, ChemDFM-R, shows promising reasoning capabilities as well as advanced performance in multiple chemical benchmarks and can provide high-quality rationale, helping researchers deeply understand and verify its answer. In short, the contributions of this work are threefold:

- We developed a toolkit to identify the functional groups of molecules and the changes of functional groups during reactions. Using this toolkit, we built a 101-billion-token domain pretraining corpus, ChemFG, which encodes atomized **f**unctional-**g**roup–level chemical knowledge.
- We proposed a mix-sourced distillation method to decompose the reasoning capabilities into three components, which are enhanced separately. This method initializes the model's reasoning ability under limited resources. With subsequent reinforcement learning, we achieve a chemical reasoning LLM, ChemDFM-R.
- Extensive experiments demonstrate the promising chemical reasoning capability of ChemDFM-R. The created model achieves outstanding performance and manages to generate clear and rational rationales, which significantly boost the reliability and interpretability of the final answer.

2 ChemFG

In the field of chemistry, functional groups serve as the bridge between molecular structures, properties, and reactivities, making them one of the most critical intermediate reasoning steps in chemical reasoning. As demonstrated in Figure 1, functional groups directly influence the properties of molecules and determine the types of reactions that can take place. However, existing training corpora of LLMs often lack detailed information on molecular functional groups, preventing models from directly and precisely learning this atomized chemical knowledge. Therefore, we collect a functional-group-centered domain pretraining corpus, ChemFG, which consists of data from three

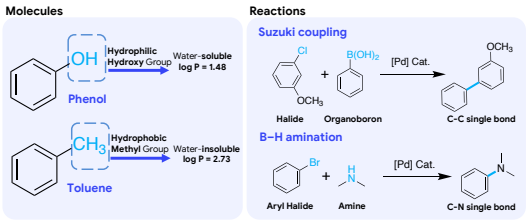

Figure 1: The influence of functional groups

Table 1: Data composition of ChemFG.

Type	Sources	#Entries	#Tokens
Literature	Internet	12M	79B
Molecules	PubChem & PubChemQC	30M	22B
Reactions	USPTO-FULL	7M	0.6B

sources: literature, molecules, and reactions. The basic statistics of ChemFG are shown in Table 1 with details provided in Appendix A.1.

2.1 Functional Group Identification

Despite the Internet-scale publicly available molecule and reaction corpora, there are no existing databases that describe the correspondence between functional groups and molecules or reactions. To tackle this issue, we develop a functional group identification toolkit based on `thermo` library[2] by extending its embedded SMARTS[3] list from 83 types of functional groups to 241 and improving its algorithms. With the help of the developed toolkit, we annotate the functional groups of all our domain-pretraining *molecule* data. Further details are provided in Appendix A.2.

As for *reactions*, we annotate the changes of functional groups during reactions with the following process. First, with the help of atom mapping annotations provided by the USPTO-FULL dataset, we identify the reaction centers as the atoms that are involved in bond changes during reactions. Based on these reaction centers and our functional group identification toolkit, we identify the functional groups of the reactants that directly participate in the reaction and those of the product that directly result from the reaction. Finally, the reaction can be described as a functional group transformation, where reacting functional groups are converted into product functional groups. Besides functional groups, there are other structural changes during reactions that are equally important, including ring breaking, ring forming, and bond changes outside functional groups. Therefore, we also construct tools to identify these changes in a similar manner.

2.2 Quality Control

To ensure the annotation quality of functional groups, we hire three chemical experts to conduct manual inspections. Firstly, all the experts agree that the extended SMARTS list has already covered the most common functional groups. For molecules, our tool's annotation accuracy of 100 random samples reaches over 90%, with errors primarily due to corner cases such as rare functional groups or complex interactions between functional groups and aromatic rings. For the annotation of reactions, our tool achieves over 80% accuracy when tested with 100 random samples. The errors mainly arise from invalid reactions or wrong atom mapping annotations.

3 ChemDFM-R

As outlined in Figure 2, the training pipeline of ChemDFM-R can be divided into two parts: 1) Domain Pretraining and Instruction Tuning (§ 3.1), where the basic general LLM is trained with atomized chemical knowledge; 2) Distillation and Reinforcement Learning (§ 3.2), where the model's chemical reasoning capability is enhanced.

3.1 Atomized Chemical Knowledge Enhancement

In this stage, our model mainly learns the atomized chemical knowledge to prepare itself with "ingredients" to "cook" the chemical rationales. Specifically, we achieve that through domain pretraining and instruction tuning.

[2] https://thermo.readthedocs.io/

[3] https://www.daylight.com/dayhtml/doc/theory/theory.smarts.html, SMiles ARbitrary Target Specification, a normalized form of SMILES.

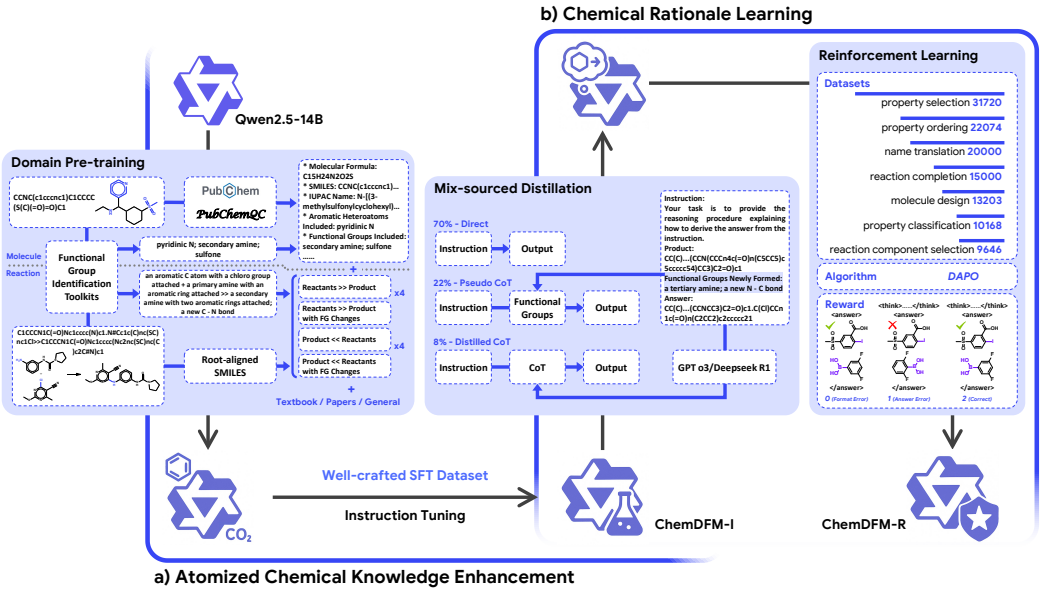

Figure 2: The overview of the training pipeline of ChemDFM-R.

Domain Pretraining. In domain pretraining, we leverage the 101-billion-token ChemFG corpus introduced in Section 2 to familiarize our model with the knowledge related to functional groups. We train our model from one of the most advanced general LLMs, Qwen2.5-14B (Yang et al., 2024a). Considering that general knowledge is also vital for Chemical LLMs, we also incorporate a substantial amount of general-domain pretraining data into our domain pretraining corpus to ensure that the model retains its general capabilities as much as possible.

Instruction Tuning. The primary goal of instruction tuning is to teach the model how to analyze the purpose and requirements of a given task and make proper use of the knowledge learned in the pretraining phase. However, existing instruction tuning datasets in the field of chemistry are typically derived from well-studied chemistry tasks and suffer from a severe lack of diversity of both task varieties and instruction expressions. Therefore, we construct a new instruction tuning dataset for ChemDFM-R based on the instruction tuning dataset of ChemDFM (Zhao et al., 2025b). To improve the overall task and instruction diversity, we introduce numerous new chemistry-related tasks, such as scientific paper QA, chemical property ordering, and reaction step prediction, and perform instruction-rewriting to achieve an average instruction-entry ratio of 1:50. For detailed information on the construction and composition of the instruction tuning dataset, please refer to Appendix B. To maintain the general capabilities of our model, we mixed our chemical instruction tuning data with general instruction tuning data in a 1:2 ratio. The Qwen2.5-14B model is finetuned for 2 epochs on this mixed dataset after domain pretraining, resulting in the ChemDFM-I model.

3.2 Chemical Rationale Learning

The primary goal of this stage is to teach the model how to reason with the atomized knowledge it has acquired. Chemical reasoning requires a deep understanding of chemical principles and logic, as well as the capability to apply them for analysis. These capabilities can not be learned or induced from general-domain reasoning training. Therefore, we propose a chemical rationale learning pipeline to specifically enhance the chemical reasoning capabilities of LLMs based on distillation and reinforcement learning.

Mix-Sourced Distillation. We leverage distillation to prevent the early unstable cold start phase of reinforcement learning. It could illustrate the reasoning patterns to the model and build up its basic reasoning capabilities.

Specifically, the entries in the distillation dataset come from three sources, each of which corresponds to part of the abilities required for chemical reasoning: 1) the instruction tuning dataset of ChemDFM-

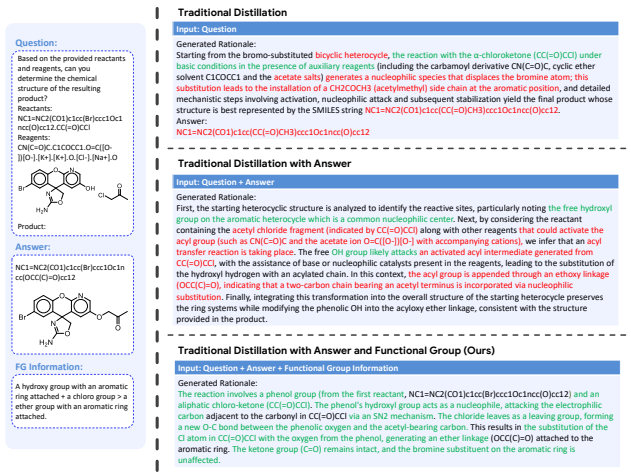

Figure 3: Comparison of rationales generated by o3-mini with and without additional input information. We mark the correct analyses in the rationale as green, while the wrong ones as red. For more examples and detailed analyses, please refer to Appendix C.

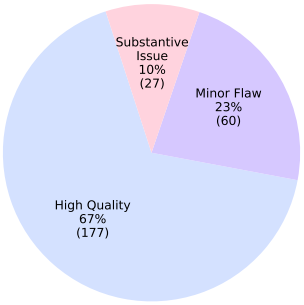

Figure 4: Human validation result of teachers' rationales. "Minor Flaw" is referred to as acceptable flaws, such as skipping reasoning steps or missing possibilities. "Substantive Issue" means severe logic errors or nonsense reasoning.

R (∼70%) to maintain basic chemical knowledge and prevent catastrophic forgetting; 2) pseudo-reasoning data describing the functional groups of involved molecules or reactions (∼22%) and highlighting vital intermediate reasoning steps and functional group analyses; 3) teachers' rationales from DeepSeek-R1 and o3-mini (∼8%) which introduce general reasoning patterns to the model and initiate its reasoning capabilities.

To improve the quality and efficiency of the teacher's rationales in the chemical domain, instead of asking teacher models to generate rationales from scratch, we provide them with rich additional information. Specifically, the teacher models are provided with the question instruction, the ground truth answer, and the functional group information of the molecules and reactions in the question. Comparison of the rationales generated by DeepSeek-R1 with and without the additional information is illustrated in Figure 3. The rationales generated with full additional information are significantly more valid and in-depth than the other two. More examples and detailed analysis of the rationale generation are given in Appendix C.

To validate the quality of the teachers' rationales generated by our method, we hired three chemical experts to perform manual inspection. According to the results illustrated in Figure 4, the quality of most generated rationales is acceptable and only ∼10% of rationales contain substantive issues. Considering the opportunity to correct errors in the following reinforcement learning stage and the difficulty of accurately filtering out the limited low-quality samples, we directly leverage all the generated data for the distillation training.

Similar to instruction tuning, we mix our mix-sourced distillation dataset with general data in a 1:2 ratio. The general data are also sampled from multiple sources, where ∼92% of the entries are sampled from the general data for instruction tuning of ChemDFM-R and ∼8% are from AM-Deepseek-R1-Distill-1.4M (Zhao et al., 2025a). The ChemDFM-I model is finetuned for one epoch on this mixed dataset.

Reinforcement Learning. After distillation, reinforcement learning (RL) is leveraged to further enhance the reasoning capabilities of our model. The composition of the RL dataset is illustrated in Figure 2, while more details of our reinforcement learning process are illustrated in Appendix D.

4 Experimental Results

We first evaluate ChemDFM-R with multiple baselines on benchmarks specifically designed for assessing the chemical capabilities of LLMs (§ 4.1). Then, to highlight the importance and ef-

Table 2: Benchmark results on SciKnowEval and ChemEval. "mol." stands for "molecule" and "react." stands for "reaction". The best performance for each task is indicated using **boldface**. * We use PRS (Peng et al., 2025) to balance the different scales of the scores on different tasks in the ChemEval benchmark.

Model	SciKnowEval				ChemEval*			
	text	mol.	react.	all	text	mol.	react.	all
Qwen2.5-14B-Instruct	**0.77**	0.36	0.72	0.61	0.78	0.24	0.43	0.55
ChemDFM-I	**0.77**	0.50	**0.95**	0.69	**0.80**	0.67	0.56	0.70
ChemDFM-R	**0.77**	**0.52**	**0.95**	**0.70**	**0.80**	**0.85**	**0.63**	**0.76**

fectiveness of chemical reasoning, we demonstrate its capability in facilitating reliable human-AI collaboration (§ 4.2).

4.1 Benchmark Evaluation

We evaluate ChemDFM-R and the baseline models on two of the most popular and comprehensive benchmarks specifically designed for assessing the chemical capabilities of LLMs: SciKnowEval (Feng et al., 2024) and ChemEval (Huang et al., 2024). Given the large number of tasks included in SciKnowEval (19 tasks) and ChemEval (36 tasks), to facilitate fair and clear comparison, we categorized the tasks into three groups: text-centric, molecule-centric, and reaction-centric tasks. Details of the task categorization are provided in the Appendix F.

4.1.1 Performance Comparison with Baselines

First, we show the effectiveness of our training pipeline by comparing the performances of ChemDFM-R with those of 1) Qwen2.5-14B-Instruct (Yang et al., 2024a), which is the general-domain instruction tuning model of Qwen2.5-14B, and 2) ChemDFM-I, which incorporates atomized chemical knowledge enhancement but precedes the stage of chemical rationale learning. The quantitative results are illustrated in Table 2, while examples of the ChemDFM-R's rationales are analyzed in Appendix E.

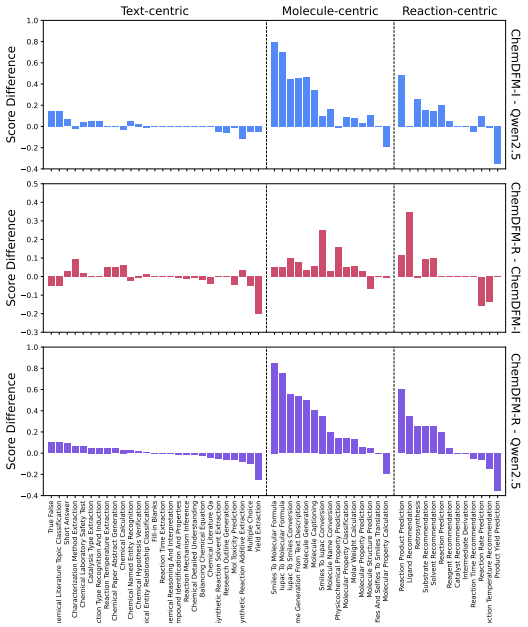

Figure 5: The performance change for all the individual tasks in SciKnowEval and ChemEval between Qwen2.5-14B-Instruct, ChemDFM-I, and ChemDFM-R.

As showcased in Table 2, ChemDFM-R consistently outperforms Qwen2.5-14B-Instruct on both SciKnowEval and ChemEval, demonstrating that our specialization pipeline has successfully improved the model's chemical capabilities. Specifically, the performances on text-centric tasks remain almost intact while those on molecule-centric and reaction-centric tasks increase significantly, leading to a large boost in the overall performance. This proves that our method manages to improve the chemical capabilities of LLM while largely maintaining its abilities in understanding natural language.

When taking the ChemDFM-I model into consideration, we observe a clear performance improvement trend from Qwen2.5-14B-Instruct to ChemDFM-I and further to ChemDFM-R. This demonstrates that both the atomized chemical knowledge enhancement stage and the chemical rationale learning stage are crucial in achieving the final performance improvement. The atomized chemical knowledge enhancement stage enhances the model's chemical knowledge, while the

Table 3: Benchmark results on SciKnowEval and ChemEval. "mol." stands for "molecule" and "react." stands for "reaction". The best performance for each task is indicated using **boldface**, while the second-best is indicated using underline. * We use PRS (Peng et al., 2025) to balance the different scales of the scores on different tasks in the ChemEval benchmark.

Model	SciKnowEval				ChemEval*			
	text	mol.	react.	all	text	mol.	react.	all
MolInst	0.69	0.38	0.42	0.55	0.47	0.16	0.09	0.29
ChemLLM-20B-DPO	0.74	0.38	0.88	0.62	0.65	0.25	0.18	0.42
ChemDFM-13B-v1.0	0.70	0.43	0.85	0.62	0.62	0.42	0.34	0.49
ChemDFM-8B-v1.5	0.72	0.46	0.87	0.64	0.27	0.13	0.18	0.21
GPT-4o	0.76	0.45	0.45	0.61	**0.83**	0.35	0.53	0.63
Qwen3-14B (no think)	0.77	0.35	0.80	0.61	<u>0.82</u>	0.25	0.27	0.53
DeepSeek-R1	0.80	0.31	0.83	0.62	0.81	0.20	0.48	0.58
Qwen3-14B (think)	**0.87**	0.41	0.88	<u>0.70</u>	0.79	0.25	0.41	0.56
o4-mini	<u>0.81</u>	**0.57**	**0.97**	**0.74**	0.78	<u>0.61</u>	<u>0.54</u>	<u>0.67</u>
ChemDFM-R	0.77	<u>0.52</u>	<u>0.95</u>	<u>0.70</u>	0.80	**0.85**	**0.63**	**0.76**

chemical rationale learning stage teaches the model how to conduct plausible reasoning with this knowledge.

Furthermore, Figure 5 illustrates the performance changes across individual tasks. The results clearly show that most tasks benefit from our training pipeline, especially the molecule-centric tasks and reaction-centric tasks. Moreover, the two training stages provide complementary gains across different tasks, enabling the final model to achieve superior results on a broader range of tasks. Notably, among the tasks where ChemDFM-R does not surpass Qwen2.5-14B-Instruct, a substantial proportion involves numerical prediction, such as Yield Extraction, Molecular Property Calculation, and Product Yield Prediction. In fact, all the molecule-centric and reaction-centric tasks where ChemDFM-R falls short of Qwen2.5-14B-Instruct are those involving numerical reasoning and prediction. This pattern suggests that the numerical calculation and prediction abilities of ChemDFM-R are relatively weak, highlighting a potential direction for further improvements.

4.1.2 Performance Comparison with Advanced LLMs

To further demonstrate the prowess of ChemDFM-R, we compare it with three sets of models: 1) existing chemical LLMs, including MolInst (Fang et al., 2024), ChemLLM (Zhang et al., 2024a), and ChemDFM (Zhao et al., 2025b); 2) advanced non reasoning LLMs in the general domain, including GPT-4o (Hurst et al., 2024) and Qwen3-14B (no think) (Yang et al., 2025); 3) advanced reasoning LLMs in the general domain, including DeepSeek-R1 (Guo et al., 2025), Qwen3-14B (think) (Yang et al., 2025), and o4-mini (OpenAI, 2025a). The experimental results are illustrated in Table 3. For detailed performances of individual tasks, please refer to Appendix F.

As shown in Table 3, ChemDFM-R significantly outperforms both the general-domain LLMs and domain-specific LLMs of similar size, especially in the molecule-centric and reaction-centric tasks. Specifically, it even surpasses Qwen3-14B, the next-generation model in the same series as our base model Qwen2.5-14B. When compared to cutting-edge LLMs, ChemDFM-R achieves better performance than GPT-4o and DeepSeek-R1, while demonstrating competitive results relative to o4-mini. Considering the tiny size of our model, this result strongly demonstrates the prowess of ChemDFM-R and the effectiveness of our specialization process.

4.1.3 Ablation Study about Mix-Sourced Distillation

To validate the effectiveness of our newly designed mix-sourced distillation method, we conduct an ablation study by gradually simplifying the composition of the distillation dataset. The results are shown in Table 4. The results prove that the traditional distillation method (row 2) struggles to achieve positive impacts on performance in the chemical domain. It even underperforms the "zero"

Table 4: Ablation study results on SciKnowEval and ChemEval. "No Thinking" denotes the data source of the instruction-tuning dataset, "Pseudo" denotes the pseudo-reasoning data source, and "Distilled" denotes the teacher's rationale data source. The best performance for each task is indicated using **boldface**. * We use PRS (Peng et al., 2025) to balance the different scales of the scores on different tasks in the ChemEval benchmark.

Data Source for Distillation			SciKnowEval				ChemEval*			
No Thinking	Pseudo	Distilled	text	mol.	react.	all	text	mol.	react.	all
✗	✗	✗	**0.77**	0.50	0.94	0.69	0.76	0.71	0.61	0.71
✗	✗	✔	0.75	0.50	0.88	0.67	0.72	0.69	**0.65**	0.69
✔	✗	✔	**0.77**	0.50	0.92	0.69	0.78	0.83	0.63	0.75
✔	✔	✔	**0.77**	**0.52**	**0.95**	**0.70**	**0.80**	**0.85**	0.63	**0.76**

method (row 1) proposed by Deepseek-R1, where there is no distillation stage before reinforcement learning. With the help of data sampled from the instruction-tuning dataset to maintain chemical capabilities and knowledge (row 3), the model's performance gets boosted significantly. Moreover, the pseudo-reasoning data further help the model to achieve higher performance (row 4), which corresponds to the final setting of our proposed mix-sourced distillation method.

4.2 Reliable Human-AI Collaboration

Another important advantage of ChemDFM-R's reasoning capability is that it allows humans to verify the correctness of answers, identify and correct errors, and discover new insights or perspectives. This enables more practical, reliable, and flexible human-AI collaboration. In this section, we demonstrate the prowess of ChemDFM-R to facilitate reliable human-AI collaboration through examples. Specifically, an example is showcased in Figure 6, while more examples are illustrated in Appendix G.

To make our example more realistic, we design our conversation topic according to a newly published chemical research paper, Li et al. (2025). It is worth noticing that this paper was published in 2025, so it is impossible for ChemDFM-R to encounter this paper during either the pretraining of the base model, Qwen2.5-14B, or our domain-pretraining process. To demonstrate the potential of ChemDFM-R, we assume the role of a researcher seeking a new research inspiration and engage the model in a dialogue about the subfield to which this paper belongs.


Turn1: What is oxygen evolution reaction (OER)? Please propose a reasonable mechanism of heterogeneous OER under acidic conditions.

<think>
To derive the answer, one starts by defining the oxygen evolution reaction (OER) as the electrochemical process that converts water into molecular oxygen, which is a critical step in water splitting. Recognizing that OER can occur under both acidic and basic conditions, the focus is on the mechanism under acidic conditions, where the reaction involves protons (H+) and water molecules. **The process is typically facilitated by a catalyst, often a transition metal oxide, which provides active sites for the reaction. The mechanism is then broken down into several steps: first, the adsorption of water molecules onto the catalyst surface, followed by the formation of an intermediate species such as an adsorbed hydroxyl group (OH–) or a water-derived species. Subsequent steps involve the transfer of protons and electrons, leading to the formation of an oxygen-oxygen bond, which is a key step in the reaction. Finally, the desorption of molecular oxygen (O2) from the catalyst completes the cycle.** This sequence of adsorption, intermediate formation, bond formation, and desorption is consistent with the known electrochemical steps in OER under acidic conditions, and it is supported by experimental observations and theoretical models.
</think>
<answer>
The oxygen evolution reaction (OER) is an electrochemical process that involves the conversion of water into molecular oxygen (O2) and protons (H+). In heterogeneous OER under acidic conditions, the reaction typically occurs on a solid catalyst surface. The mechanism can be described as follows:

1. **Water adsorption**: Water molecules (H2O) adsorb onto the catalyst surface.
2. **Proton transfer**: Protons (H+) are transferred from the adsorbed water molecules to the catalyst surface, forming hydroxyl (OH-) groups.
3. **Oxygen adsorption**: The hydroxyl groups further react to form adsorbed oxygen species (O*), which are intermediates in the reaction.
4. **Oxygen evolution**: The adsorbed oxygen species combine to form molecular oxygen (O2), which desorbs from the catalyst surface and enters the solution.

The overall reaction can be represented as:

2H2O → O2 + 4H+ + 4e-
</answer>

Turn2: Since you mentioned that some transition metal oxides possess catalytic properties, can you recommend some specific metal oxides in detail?

<think>
To determine which transition metal oxides exhibit catalytic properties for the oxygen evolution reaction (OER), one considers the electronic structure and surface reactivity of these materials. **The oxides of metals such as iridium (Ir), ruthenium (Ru), and cobalt (Co) are known to be effective catalysts due to their favorable electronic properties and ability to stabilize reaction intermediates. Iridium oxide (IrO2) is *particularly notable* for its high activity and stability under acidic conditions, making it a widely used catalyst in OER applications. Ruthenium oxide (RuO2) also demonstrates excellent catalytic performance, while cobalt oxide (Co3O4) has been explored for its cost-effectiveness and moderate activity. These metal oxides are incorporated into electrochemical cells, where they facilitate the adsorption of water molecules, the formation of oxygen-containing intermediates, and the subsequent bond formation leading to O2 evolution.** The selection of these materials is supported by extensive experimental data and theoretical calculations that highlight their ability to enhance the efficiency of the OER process.
</think>
<answer>
Some transition metal oxides that possess catalytic properties for the oxygen evolution reaction (OER) include iridium oxide (IrO2), ruthenium oxide (RuO2), and cobalt oxide (Co3O4). These metal oxides are commonly used as catalysts in electrochemical cells for water splitting and other applications. They exhibit high catalytic activity under acidic conditions, making them suitable for OER. The catalytic activity of these metal oxides is attributed to their electronic structure and ability to stabilize reaction intermediates during the OER process.
</answer>

Turn3: I noticed that you mentioned iridium oxide (IrO2) is particularly notable, but iridium, as a noble metal, is relatively expensive. Can you devise a plan to reduce the cost while still maintaining good catalytic activity?

<think>
To address the high cost of noble metal catalysts like iridium oxide while maintaining catalytic activity, one can explore strategies that reduce their usage or enhance their efficiency. **One approach involves incorporating these metals into composite materials, where they are combined with cheaper transition metal oxides such as cobalt or nickel. By forming mixed metal oxides or heterostructures, the expensive metals can be distributed more efficiently, leveraging their catalytic properties while minimizing their overall amount. Additionally, optimizing the morphology and surface area of the catalysts, such as by creating nanostructures or thin films, can increase the active sites available for the reaction, thereby enhancing performance without requiring larger quantities of the noble metals. Furthermore, doping or alloying these metals with other elements can modify their electronic properties, improving their catalytic activity and reducing the necessary loading.** These strategies collectively aim to balance cost-effectiveness with catalytic efficiency in the oxygen evolution reaction.
</think>
<answer>
To reduce the cost of iridium oxide (IrO2) while maintaining good catalytic activity, one approach is to incorporate it into a composite material with a less expensive metal oxide, such as cobalt oxide (Co3O4) or nickel oxide (NiO). This composite material can exhibit enhanced catalytic properties due to the synergistic effects between the two metal oxides. Another strategy is to optimize the morphology and surface area of the catalyst, which can improve its activity and reduce the amount of IrO2 required. Additionally, doping IrO2 with other metal ions, such as iron (Fe) or manganese (Mn), can modify its electronic properties and enhance its catalytic performance. These approaches can help reduce the cost of IrO2 while still achieving good catalytic activity for the oxygen evolution reaction (OER).
</answer>

Figure 6: An example of reliable human-AI collaboration using ChemDFM-R. This conversation is inspired by Li et al. (2025). This example illustrates a process of research inspiration seeking with the help of ChemDFM-R.

First, as a researcher seeking inspiration, we ask ChemDFM-R to introduce the oxygen evolution reaction (OER) briefly, including the definition and mechanism of it. Although the answer itself is

a relatively rigid response to the question, the model's rationale reveals interesting insights. In its rationale, ChemDFM-R mentions that OER requires a transition metal oxide catalyst, which often presents valuable opportunities for further research. Therefore, we further ask it to give more detailed recommendations for the catalysts. As a response, ChemDFM-R proposes multiple different oxides, which is a wide range for us to dig into. However, in its rationale, ChemDFM-R itself says that "iridium oxide (IrO2) is *particularly notable* for its ...", which is very inspiring. Since it is well known that iridium-based compounds are often very expensive, a natural follow-up question arises: how can we optimize this catalyst to reduce its cost while maintaining its catalytic performance? Surprisingly, ChemDFM-R manages to propose the initial ideas that align closely with the ideas presented in Li et al. (2025), "forming mixed metal oxides or heterostructures" and "optimizing the morphology and surface area of the catalysts". At this point, a broad research direction has taken shape.

It is worth noticing that nearly all the inspirations are drawn from the rationale of ChemDFM-R, which demonstrates the significance and value of ChemDFM-R's ability to generate reasoning. This example shows that, with the enhanced chemical knowledge and strong chemical reasoning capabilities, ChemDFM-R has the potential to facilitate reliable human-AI collaboration, thereby advancing AI-driven research and applications. More examples involving error correction and answer improvement with the help of rationales are demonstrated in Appendix G.

5 Related Work

General Domain Reasoning LLMs. Shortly after the emergence of LLMs, their remarkable reasoning capabilities were discovered by Kojima et al. (2022) and explored by works such as ToT (Yao et al., 2023) and PAL (Gao et al., 2023). Recently, OpenAI-o1 (Jaech et al., 2024) followed by DeepSeek-R1 (Guo et al., 2025) and Kimi K1.5 (Team et al., 2025) demonstrated the prowess of reasoning models and the method to enhance LLMs' reasoning capabilities using reinforcement learning-based pipelines. Subsequently, many studies have focused on improving the reasoning capabilities of models in various general domains, primarily in mathematics and coding. For example, Shao et al. (2024) and Zhang et al. (2024b) have further proven and discussed the effectiveness of reinforcement learning in terms of enhancing models' reasoning capabilities, while Dou et al. (2024) and Zhang et al. (2025c) have explored better reward functions in mathematics and coding.

Chemical LLMs. The specialization of LLMs has become one of the most popular research areas after the emergence of general-use LLMs, including the development of chemical LLMs. LlaSMol (Yu et al., 2024) and Mol-Instruct (Fang et al., 2024) construct a chemical instruction tuning dataset and develop models that could excel in multiple chemical tasks, while extensive training with only chemical tasks has led to a substantive loss of natural language capabilities and task generalization ability in these models. Shortly after, Zhang et al. (2024a) leveraged high-quality instruction tuning and developed ChemLLM, which has acquired advanced chemical capabilities while retaining a considerable level of general language abilities. Furthermore, ChemDFM (Zhao et al., 2025b) achieved stronger chemical and generalization capabilities through domain pretraining and instruction tuning with both chemical data and general-domain data. It is worth noticing that the data used in previous work overlooks the intrinsic chemical essence, which is crucial for LLMs to master reasoning with chemical intuition and principles. To tackle this issue, we construct a function-group-centric domain pretraining corpus to introduce such atomized chemical knowledge to LLMs. Recently, there has been some work building reasoning models for specific chemical tasks, such as retrosynthesis (Zhang et al., 2025a), but a general chemical reasoning model is still absent.

6 Conclusion

In this work, we have developed a chemical reasoning LLM, ChemDFM-R, by tackling both the limitations in understanding atomized chemical knowledge and the domain-specific reasoning logic. By incorporating atomized knowledge about molecular functional groups and their changes during reactions into the pretraining corpus, and applying a mix-sourced distillation approach before reinforcement learning, we have enhanced the model's ability to reason efficiently and effectively in chemistry. Our extensive experiments demonstrate that ChemDFM-R significantly improves chemical problem-solving and reasoning capabilities, making it a valuable tool for facilitating reliable human-AI collaboration in chemistry and advancing AI-driven research and applications.

REFERENCES

Josh Achiam, Steven Adler, Sandhini Agarwal, Lama Ahmad, Ilge Akkaya, Florencia Leoni Aleman, Diogo Almeida, Janko Altenschmidt, Sam Altman, Shyamal Anadkat, et al. Gpt-4 technical report. *arXiv preprint arXiv:2303.08774*, 2023.

Luis M Antunes, Keith T Butler, and Ricardo Grau-Crespo. Crystal structure generation with autoregressive large language modeling. *Nature Communications*, 15(1):10570, 2024.

Tom Brown, Benjamin Mann, Nick Ryder, Melanie Subbiah, Jared D Kaplan, Prafulla Dhariwal, Arvind Neelakantan, Pranav Shyam, Girish Sastry, Amanda Askell, et al. Language models are few-shot learners. *Advances in neural information processing systems*, 33:1877–1901, 2020.

Mark Chen, Jerry Tworek, Heewoo Jun, Qiming Yuan, Henrique Ponde De Oliveira Pinto, Jared Kaplan, Harri Edwards, Yuri Burda, Nicholas Joseph, Greg Brockman, et al. Evaluating large language models trained on code. *arXiv preprint arXiv:2107.03374*, 2021.

Gheorghe Comanici, Eric Bieber, Mike Schaekermann, Ice Pasupat, Noveen Sachdeva, Inderjit Dhillon, Marcel Blistein, Ori Ram, Dan Zhang, Evan Rosen, et al. Gemini 2.5: Pushing the frontier with advanced reasoning, multimodality, long context, and next generation agentic capabilities. *arXiv preprint arXiv:2507.06261*, 2025.

Hanjun Dai, Chengtao Li, Connor Coley, Bo Dai, and Le Song. Retrosynthesis prediction with conditional graph logic network. *Advances in Neural Information Processing Systems*, 32, 2019.

Shihan Dou, Yan Liu, Haoxiang Jia, Limao Xiong, Enyu Zhou, Wei Shen, Junjie Shan, Caishuang Huang, Xiao Wang, Xiaoran Fan, et al. Stepcoder: Improve code generation with reinforcement learning from compiler feedback. *arXiv preprint arXiv:2402.01391*, 2024.

Yin Fang, Xiaozhuan Liang, Ningyu Zhang, Kangwei Liu, Rui Huang, Zhuo Chen, Xiaohui Fan, and Huajun Chen. Mol-instructions: A large-scale biomolecular instruction dataset for large language models. In *ICLR*. OpenReview.net, 2024. URL https://openreview.net/pdf?id=Tlsdsb6l9n.

Kehua Feng, Keyan Ding, Weijie Wang, Xiang Zhuang, Zeyuan Wang, Ming Qin, Yu Zhao, Jianhua Yao, Qiang Zhang, and Huajun Chen. Sciknoweval: Evaluating multi-level scientific knowledge of large language models. *arXiv preprint arXiv:2406.09098*, 2024.

Luyu Gao, Aman Madaan, Shuyan Zhou, Uri Alon, Pengfei Liu, Yiming Yang, Jamie Callan, and Graham Neubig. Pal: Program-aided language models. In *International Conference on Machine Learning*, pp. 10764–10799. PMLR, 2023.

Daya Guo, Dejian Yang, Haowei Zhang, Junxiao Song, Ruoyu Zhang, Runxin Xu, Qihao Zhu, Shirong Ma, Peiyi Wang, Xiao Bi, et al. Deepseek-r1: Incentivizing reasoning capability in llms via reinforcement learning. *arXiv preprint arXiv:2501.12948*, 2025.

Dan Hendrycks, Collin Burns, Steven Basart, Andy Zou, Mantas Mazeika, Dawn Song, and Jacob Steinhardt. Measuring massive multitask language understanding. *arXiv preprint arXiv:2009.03300*, 2020.

Yuqing Huang, Rongyang Zhang, Xuesong He, Xuyang Zhi, Hao Wang, Xin Li, Feiyang Xu, Deguang Liu, Huadong Liang, Yi Li, et al. Chemeval: a comprehensive multi-level chemical evaluation for large language models. *arXiv preprint arXiv:2409.13989*, 2024.

Binyuan Hui, Jian Yang, Zeyu Cui, Jiaxi Yang, Dayiheng Liu, Lei Zhang, Tianyu Liu, Jiajun Zhang, Bowen Yu, Keming Lu, et al. Qwen2. 5-coder technical report. *arXiv preprint arXiv:2409.12186*, 2024.

Aaron Hurst, Adam Lerer, Adam P Goucher, Adam Perelman, Aditya Ramesh, Aidan Clark, AJ Ostrow, Akila Welihinda, Alan Hayes, Alec Radford, et al. Gpt-4o system card. *arXiv preprint arXiv:2410.21276*, 2024.

Aaron Jaech, Adam Kalai, Adam Lerer, Adam Richardson, Ahmed El-Kishky, Aiden Low, Alec Helyar, Aleksander Madry, Alex Beutel, Alex Carney, et al. Openai o1 system card. *arXiv preprint arXiv:2412.16720*, 2024.

Wengong Jin, Connor Coley, Regina Barzilay, and Tommi Jaakkola. Predicting organic reaction outcomes with weisfeiler-lehman network. *Advances in neural information processing systems*, 30, 2017.

Takeshi Kojima, Shixiang Shane Gu, Machel Reid, Yutaka Matsuo, and Yusuke Iwasawa. Large language models are zero-shot reasoners. *Advances in neural information processing systems*, 35: 22199–22213, 2022.

Gengnan Li, Adyasa Priyadarsini, Zhenhua Xie, Sinwoo Kang, Yuzi Liu, Xiaobo Chen, Shyam Kattel, and Jingguang G Chen. Achieving higher activity of acidic oxygen evolution reaction using an atomically thin layer of iro x over co3o4. *Journal of the American Chemical Society*, 147(8): 7008–7016, 2025.

Maho Nakata and Tomomi Shimazaki. Pubchemqc project: a large-scale first-principles electronic structure database for data-driven chemistry. *Journal of chemical information and modeling*, 57(6): 1300–1308, 2017.

OpenAI. Introducing openai o3 and o4-mini, 2025a. URL https://openai.com/index/introducing-o3-and-o4-mini.

OpenAI. Openai o3-mini, jan 2025b. URL https://openai.com/index/introducing-o3-and-o4-mini.

Jing Peng, Yucheng Wang, Bohan Li, Yiwei Guo, Hankun Wang, Yangui Fang, Yu Xi, Haoyu Li, Xu Li, Ke Zhang, Shuai Wang, and Kai Yu. A survey on speech large language models for understanding, 2025. URL https://arxiv.org/abs/2410.18908.

Nadine Schneider, Nikolaus Stiefl, and Gregory A Landrum. What's what: The (nearly) definitive guide to reaction role assignment. *Journal of chemical information and modeling*, 56(12):2336–2346, 2016.

Zhihong Shao, Peiyi Wang, Qihao Zhu, Runxin Xu, Junxiao Song, Xiao Bi, Haowei Zhang, Mingchuan Zhang, YK Li, Yang Wu, et al. Deepseekmath: Pushing the limits of mathematical reasoning in open language models. *arXiv preprint arXiv:2402.03300*, 2024.

Anuroop Sriram, Benjamin Miller, Ricky TQ Chen, and Brandon Wood. Flowllm: Flow matching for material generation with large language models as base distributions. *Advances in Neural Information Processing Systems*, 37:46025–46046, 2024.

Qian Tan, Dongzhan Zhou, Peng Xia, Wanhao Liu, Wanli Ouyang, Lei Bai, Yuqiang Li, and Tianfan Fu. Chemmllm: Chemical multimodal large language model. *arXiv preprint arXiv:2505.16326*, 2025.

Ross Taylor, Marcin Kardas, Guillem Cucurull, Thomas Scialom, Anthony Hartshorn, Elvis Saravia, Andrew Poulton, Viktor Kerkez, and Robert Stojnic. Galactica: A large language model for science. *arXiv preprint arXiv:2211.09085*, 2022.

Gemini Team, Rohan Anil, Sebastian Borgeaud, Jean-Baptiste Alayrac, Jiahui Yu, Radu Soricut, Johan Schalkwyk, Andrew M Dai, Anja Hauth, Katie Millican, et al. Gemini: a family of highly capable multimodal models. *arXiv preprint arXiv:2312.11805*, 2023.

Kimi Team, Angang Du, Bofei Gao, Bowei Xing, Changjiu Jiang, Cheng Chen, Cheng Li, Chenjun Xiao, Chenzhuang Du, Chonghua Liao, et al. Kimi k1. 5: Scaling reinforcement learning with llms. *arXiv preprint arXiv:2501.12599*, 2025.

Yuwei Wan, Yixuan Liu, Aswathy Ajith, Clara Grazian, Bram Hoex, Wenjie Zhang, Chunyu Kit, Tong Xie, and Ian Foster. Sciqag: A framework for auto-generated science question answering dataset with fine-grained evaluation, 2024. URL https://arxiv.org/abs/2405.09939.

Yubo Wang, Xueguang Ma, Ge Zhang, Yuansheng Ni, Abhranil Chandra, Shiguang Guo, Weiming Ren, Aaran Arulraj, Xuan He, Ziyan Jiang, et al. Mmlu-pro: A more robust and challenging multi-task language understanding benchmark. *Advances in Neural Information Processing Systems*, 37: 95266–95290, 2024.

Zhenqin Wu, Bharath Ramsundar, Evan N Feinberg, Joseph Gomes, Caleb Geniesse, Aneesh S Pappu, Karl Leswing, and Vijay Pande. Moleculenet: a benchmark for molecular machine learning. *Chemical science*, 9(2):513–530, 2018.

Tong Xie, Yuwei Wan, Wei Huang, Zhenyu Yin, Yixuan Liu, Shaozhou Wang, Qingyuan Linghu, Chunyu Kit, Clara Grazian, Wenjie Zhang, et al. Darwin series: Domain specific large language models for natural science. *arXiv preprint arXiv:2308.13565*, 2023.

An Yang, Baosong Yang, Beichen Zhang, Binyuan Hui, Bo Zheng, Bowen Yu, Chengyuan Li, Dayiheng Liu, Fei Huang, Haoran Wei, et al. Qwen2. 5 technical report. *arXiv preprint arXiv:2412.15115*, 2024a.

An Yang, Beichen Zhang, Binyuan Hui, Bofei Gao, Bowen Yu, Chengpeng Li, Dayiheng Liu, Jianhong Tu, Jingren Zhou, Junyang Lin, et al. Qwen2. 5-math technical report: Toward mathematical expert model via self-improvement. *arXiv preprint arXiv:2409.12122*, 2024b.

An Yang, Anfeng Li, Baosong Yang, Beichen Zhang, Binyuan Hui, Bo Zheng, Bowen Yu, Chang Gao, Chengen Huang, Chenxu Lv, et al. Qwen3 technical report. *arXiv preprint arXiv:2505.09388*, 2025.

Shunyu Yao, Dian Yu, Jeffrey Zhao, Izhak Shafran, Tom Griffiths, Yuan Cao, and Karthik Narasimhan. Tree of thoughts: Deliberate problem solving with large language models. *Advances in neural information processing systems*, 36:11809–11822, 2023.

Weidong Yao, Ziqi Liu, Hao Ling, Hongyu Wang, Hufeng Zheng, Shao-Hua Wang, Dao-Yong Zhu, Sheng-Yong Zhang, and Xiaoming Chen. Convergent total synthesis of (-)-calidoustene. *Journal of the American Chemical Society*, 147(19):15963–15969, 2025.

Botao Yu, Frazier N Baker, Ziqi Chen, Xia Ning, and Huan Sun. Llasmol: Advancing large language models for chemistry with a large-scale, comprehensive, high-quality instruction tuning dataset. *arXiv preprint arXiv:2402.09391*, 2024.

Qiying Yu, Zheng Zhang, Ruofei Zhu, Yufeng Yuan, Xiaochen Zuo, Yu Yue, Weinan Dai, Tiantian Fan, Gaohong Liu, Lingjun Liu, et al. Dapo: An open-source llm reinforcement learning system at scale. *arXiv preprint arXiv:2503.14476*, 2025.

Di Zhang, Wei Liu, Qian Tan, Jingdan Chen, Hang Yan, Yuliang Yan, Jiatong Li, Weiran Huang, Xiangyu Yue, Wanli Ouyang, et al. Chemllm: A chemical large language model. *arXiv preprint arXiv:2402.06852*, 2024a.

Situo Zhang, Hanqi Li, Lu Chen, Zihan Zhao, Xuanze Lin, Zichen Zhu, Bo Chen, Xin Chen, and Kai Yu. Reasoning-driven retrosynthesis prediction with large language models via reinforcement learning, 2025a. URL https://arxiv.org/abs/2507.17448.

Yu Zhang, Yang Han, Shuai Chen, Ruijie Yu, Xin Zhao, Xianbin Liu, Kaipeng Zeng, Mengdi Yu, Jidong Tian, Feng Zhu, et al. Large language models to accelerate organic chemistry synthesis. *Nature Machine Intelligence*, pp. 1–13, 2025b.

Yuxiang Zhang, Shangxi Wu, Yuqi Yang, Jiangming Shu, Jinlin Xiao, Chao Kong, and Jitao Sang. o1-coder: an o1 replication for coding. *arXiv preprint arXiv:2412.00154*, 2024b.

Zhenru Zhang, Chujie Zheng, Yangzhen Wu, Beichen Zhang, Runji Lin, Bowen Yu, Dayiheng Liu, Jingren Zhou, and Junyang Lin. The lessons of developing process reward models in mathematical reasoning. *arXiv preprint arXiv:2501.07301*, 2025c.

Han Zhao, Haotian Wang, Yiping Peng, Sitong Zhao, Xiaoyu Tian, Shuaiting Chen, Yunjie Ji, and Xiangang Li. 1.4 million open-source distilled reasoning dataset to empower large language model training. *arXiv preprint arXiv:2503.19633*, 2025a.

Zihan Zhao, Bo Chen, Jingpiao Li, Lu Chen, Liyang Wen, Pengyu Wang, Zichen Zhu, Danyang Zhang, Yansi Li, Zhongyang Dai, et al. Chemdfm-x: towards large multimodal model for chemistry. *Science China Information Sciences*, 67(12):220109, 2024.

Zihan Zhao, Da Ma, Lu Chen, Liangtai Sun, Zihao Li, Yi Xia, Bo Chen, Hongshen Xu, Zichen Zhu, Su Zhu, et al. Developing chemdfm as a large language foundation model for chemistry. *Cell Reports Physical Science*, 6(4), 2025b.

Zipeng Zhong, Jie Song, Zunlei Feng, Tiantao Liu, Lingxiang Jia, Shaolun Yao, Min Wu, Tingjun Hou, and Mingli Song. Root-aligned smiles: a tight representation for chemical reaction prediction. *Chemical Science*, 13(31):9023–9034, 2022.

Qihao Zhu, Daya Guo, Zhihong Shao, Dejian Yang, Peiyi Wang, Runxin Xu, Y Wu, Yukun Li, Huazuo Gao, Shirong Ma, et al. Deepseek-coder-v2: Breaking the barrier of closed-source models in code intelligence. *arXiv preprint arXiv:2406.11931*, 2024.

DISCLOSING OF LLM USAGE

LLMs are leveraged exclusively as an assist tool for paper writing. We only use them to help us polish the language and improve readability. They do not contribute to any of the creative work involved in this paper, such as research ideation, experiment design, data analysis, and result interpretation. Therefore, they should not be regarded as authorship or substantive contribution.

A DETAILS ABOUT CHEMFG

A.1 RAW DATA COLLECTION

Literature. Literature, including papers and textbooks, contains not only the widely accepted chemical knowledge and principles, but also the cutting-edge research in the field of chemistry. Therefore, to take full advantage of chemical literature, we collected over 12 million literature from the open Internet dated prior to January 2022. After further cleaning and deduplication, 79B tokens are obtained from it.

Molecules. Molecules are the fundamental participants in various chemical processes. Therefore, it is crucial for Chemical LLMs to understand molecular structures and properties. We manage to acquire large-scale molecule datasets from PubChem[4], one of the biggest open accessible chemical databases with more than 100M compounds. We include 30 million molecules along with their notations, descriptions (if applicable), and properties. Besides PubChem, we also leverage the PubChemQC (Nakata & Shimazaki, 2017) dataset, which contains the quantum chemical calculation results of 86M molecules from PubChem, to supplement the quantum chemical properties of these molecules, such as dipole moment and orbital energy. To diversify the final data entry, we randomize the order of the properties and use three different formats: markdown list, markdown table, and JSON dictionary to formulate the molecule data.

Reactions. Reactions are the major process in the chemical world. In ChemFG, we use the reactions from USPTO-FULL (Dai et al., 2019), one of the most comprehensive open-sourced chemical reaction databases. To avoid data leakage, we exclude the test set of USPTO-FULL, USPTO-MIT (Jin et al., 2017), and USPTO-50K (Schneider et al., 2016) according to the products of reactions. Moreover, to further enhance the data diversity, we leverage the SMILES (Simplified Molecular Input Line Entry System) augmentation method introduced in R-SMILES (Zhong et al., 2022) and achieve a total of 10 times augmentation of data. Finally, a corpus of 7 million reactions is obtained.

A.2 FUNCTIONAL GROUPS COVERAGE

The functional groups that can be recognized by our toolkit are categorized based on the heteroatoms and listed as follows:

- **Hydrocarbon Groups (7)**: alkene, alkyne, allene, cumulene, carbocation, carbanion, carbene.

[4] https://pubchem.ncbi.nlm.nih.gov/

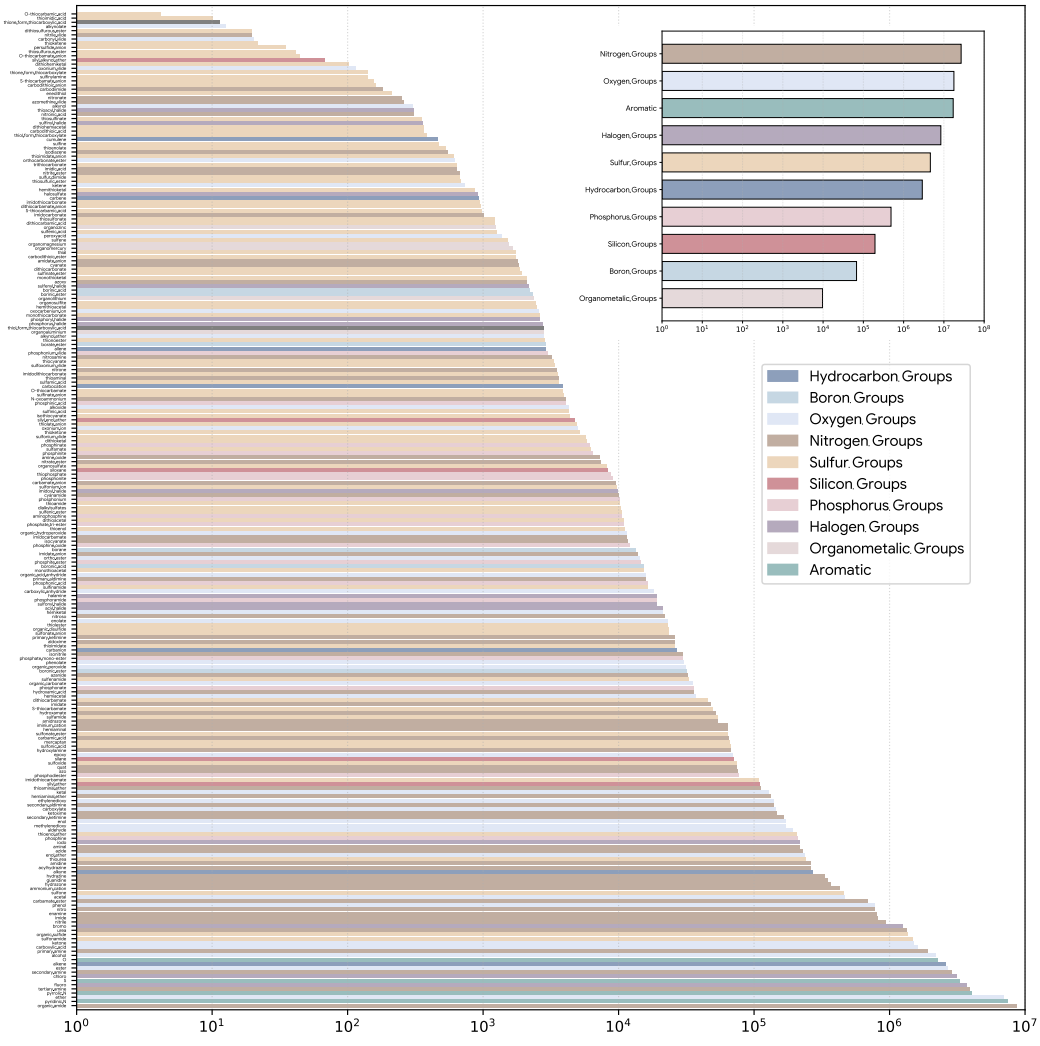

Figure 7: The distribution of the functional groups in the domain-pretraining corpus.

- **Boron Groups (6)**: borane, boronic acid, boronic ester, borinic acid, borinic ester, borate ester.
- **Oxygen Groups (36)**: alcohol, alkoxide, ether, phenol, phenolate, enol, enolate, enol ether, alkynol, alkynolate, alkynol ether, ketone, ketene, aldehyde, hemiketal, hemiacetal, ketal, acetal, carboxylic acid, carboxylate, ester, organic acid anhydride, carboxylic anhydride, organic carbonate, organic hydroperoxide, organic peroxide, peroxyacid, ortho ester, orthocarbonate ester, methylenedioxy, ethylenedioxy, oxonium ion, oxocarbenium ion, carbonyl ylide, oxonium ylide, epoxy.
- **Nitrogen Groups (62)**: primary amine, secondary amine, tertiary amine, ammonium cation, quat, amine oxide, enamine, hydroxylamine, hemiaminal, hemiaminal ether, thioaminal, thioaminal ether, aminal, primary ketimine, secondary ketimine, primary aldimine, secondary aldimine, amidine, guanidine, ketoxime, aldoxime, hydrazone, organic amide, amidate anion, imide, carbamic acid, carbamate ester, carbamate anion, azide, azo, hydrazine, acylhydrazine, amidrazone, cyanate, isocyanate, nitrile, isonitrile, cyanamide, carbodiimide, nitrate ester, nitrite ester, nitro, nitroso, nitrosamine, iminium cation, nitrone, nitronic acid, imidic acid, imidate anion, imidate, imidocarbonate, imidocarbamate, urea, azoxy, N-oxoammonium, hydroxamic acid, hydroxamate, azanide, azomethine ylide, nitrile ylide, isodiazene, nitronate.
- **Sulfur Groups (85)**: mercaptan, thiolate anion, organic sulfide, thioenol, enedithiol, thioenolate, thioenol ether, persulfide anion, organic disulfide, sulfenic acid, sulfenic ester, sulfenamide, sulfoxide, sulfone, sulfine, sulfene, sulfinylamine, sulfur diimide, sulfinic acid, sulfonic acid, sulfinate ester, sulfonate ester, sulfinate anion, sulfonate anion, thiosulfinate, thiosulfonate, thiosulfurous ester, dithiosulfurous ester, thiosulfuric ester, organosulfite, organosulfate, dialkylsulfates, sulfinamide, sulfonamide, sulfamic acid, sulfamate, sulfamide, thiocyanate, isothiocyanate, thioketone, thioketene, thial, thioamide, thiourea, hemithioketal, hemithioacetal, dithiohemiketal, dithiohemiacetal, monothioketal, monothioacetal, dithioketal, dithioacetal, carbothioic S-acid, carbothioic O-acid, thiol form thiocarboxylate, thione form thiocarboxylate, thiolester, thionoester, carbodithioic acid, carbodithioic anion, carbodithioic ester, monothiocarbonate, xanthic acid, xanthate, xanthate anion, dithiocarbonate, trithiocarbonate, O-thiocarbamic acid, S-thiocarbamic acid, O-thiocarbamate, S-thiocarbamate, O-thiocarbamate anion, S-thiocarbamate anion, thioimidic acid, thioimidate anion, thioimidate, dithiocarbamic acid, dithiocarbamate, dithiocarbamate anion, imidothiocarbonate, imidodithiocarbonate, imidothiocarbamate, sulfonium ion, sulfonium ylide, sulfoxonium ylide.
- **Silicon Groups (5)**: silane, siloxane, silyl ether, silyl enol ether, silyl alkynol ether.
- **Phosphorus Groups (17)**: phosphine, phosphonium, aminophosphine, phosphine oxide, phosphinic acid, phosphinate, phosphonic acid, phosphonate, phosphite ester, phosphinite, phosphonite, phosphodiester, phosphate mono-ester, phosphate tri-ester, phosphoramide, thiophosphate, phosphonium ylide.
- **Halogen Groups (14)**: fluoro, chloro, bromo, iodo, halamine, sulfenyl halide, sulfinyl halide, sulfonyl halide, halosulfate, phosphoryl halide, phosphorus halide, acyl halide, imidoyl halide, thioacyl halide.
- **Organometalic Groups (5)**: organolithium, organomagnesium, organoaluminium, organozinc, organomercury.
- **Aromatic (4)**: pyrrolic N, pyridinic N, aromatic O, aromatic S.

The occurrence of these functional groups in the domain-pretraining corpus is shown in Figure 7.

B Instruction Tuning Dataset

B.1 Raw Data Collection

Our instruction tuning dataset is constructed of three parts corresponding to the three main information carriers in chemistry: molecule-centric tasks, reaction-centric tasks, and knowledge-centric tasks. The distribution of instruction tuning data is shown in Figure 8.

B.1.1 MOLECULE-CENTRIC TASKS

- **Name Translation**: The name translation between SMILES, IUPAC name, and molecular formula. The data is constructed from PubChem[5].
- **Description Generation**: The molecule description task is to describe the molecule given its SMILES. The data is constructed from PubChem. We only use the high-quality descriptions that contain more than two sentences.
- **Molecule Design**: The molecule design task is the reverse task of molecule description. It requires the model to predict the SMILES given the molecule description. We use the same high-quality description data from PubChem to construct this task.
- **Property Classification**: These tasks require models to predict the value of molecular properties from a list of candidates (usually yes and no). The data is constructed from 5 of the most popular property classification datasets in MoleculeNet (Wu et al., 2018), namely BACE, BBBP, ClinTox, HIV, and Tox21.
- **Property Regression**: These tasks require the models to predict the value of molecular properties, which is a real number. Data are also from MoleculeNet, namely FreeSolv, Lipo, and QM9.
- **Property Ordering**: Provided a list of molecules, models are asked to rank them in ascending or descending order of some specific property. Raw data comes from the same source as property regression.
- **Property Selection**: Provided a list of molecules, models are asked to select the one with the highest or lowest value of some specific property. Raw data comes from the same source as property regression.

B.1.2 REACTION-CENTRIC TASKS

- **Reaction Completion**: Given an incomplete reaction, models need to complete the missing reactants, reagents, or products. Raw data comes from USPTO-Full (Dai et al., 2019), USPTO-MIT (Jin et al., 2017), and USPTO-50K (Schneider et al., 2016).
- **Step Prediction**: Given a reaction, models are required to predict the experimental procedure to conduct it in the laboratory. Raw data comes from USPTO (Dai et al., 2019).
- **Yield Prediction**: In this task, models are required to predict the yield of the given reactions. The data is constructed from the USPTO dataset.
- **Temperature Prediction**: In this task, models are required to predict the temperature that is suitable for the given reactions to conduct. The data is constructed from the USPTO dataset.
- **Reaction Component Selection**: In this task, a series of reactants and reagents is given with a list of candidate molecules. Models need to pick from the candidates the molecules that could participate in the reaction and lead to the highest yield. The data is constructed from the USPTO dataset.

B.1.3 KNOWLEDGE-CENTRIC TASKS

- **Exam Questions**: This task is composed of questions from the exams in middle school and high school. Raw data comes from the Open Internet.
- **Literature QA**: In this task, models are required to answer questions based on the given paragraph. The data is extracted from the long paragraph following the method in SciQAG (Wan et al., 2024). The raw data comes from the articles in the domain-pertaining. The articles are split into sections and then truncated into paragraphs within 2k to 3k tokens. We ask GPT-4o-mini to extract 15 keywords from each paragraph, then generate 10 question-answer pairs according to them. We adopt another LLM, Qwen2.5-14B-Instruct, to evaluate the quality of the QA pair in 4 dimensions: completeness, accuracy, reasonableness, and agnosticism. The LLM will score the QA pair from 1 to 5 using the designed prompts. QA pairs with any scores below 5 are discarded. If there are more than 1 QA pair left, the questions are asked in conversation turns.

[5] https://pubchem.ncbi.nlm.nih.gov/

- **Literature Summarization**: In this task, models are required to give a summarization of the paragraph. The summarization is generated from GPT-4o-mini from the paragraph sample.
- **Literature Translation**: In this task, models are required to translate the English paragraph into Chinese. The translation is generated from GPT-4o-mini from the paragraph sample. Since the source data consists of OCR text extracted from English articles, which is inherently noisy, we decided to discard the reverse task of translating Chinese paragraphs into English.

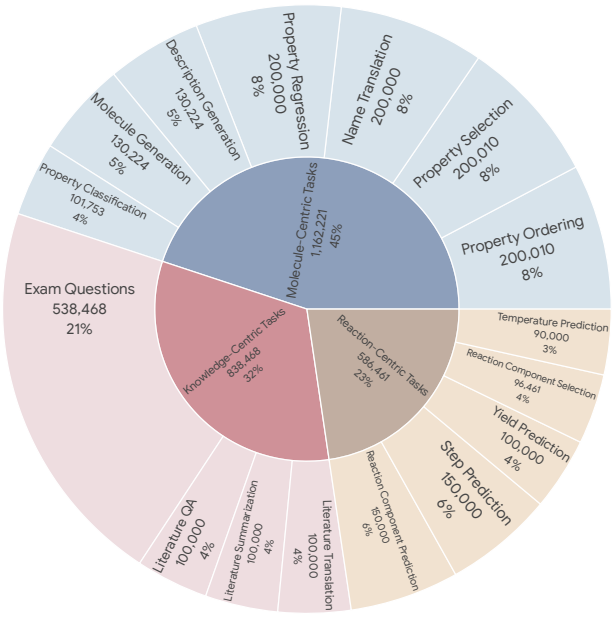

Figure 8: The distribution of instruction tuning data.

B.2 Instruction Generation

To acquire a higher generalization capability, we adopt a two-stage process to obtain as diverse a set of instructions as possible for each task. Specifically, based on the number of data entries for each task, we first manually write 5-20 seed task descriptions accordingly. Then, we ask three different models, Qwen2.5-72B-Instruct, Llama-3.1-70B-Instruct, and GPT-4o-mini, to diversify these task descriptions. Specifically, during each request, we sample 5 descriptions from all the generated descriptions and ask the model to generate 10 new descriptions using 5 different prompts one by one. Following this, we append to each of the descriptions the instructions that introduce the input of each data entry by a formatted string of Python and ask GPT-4o-mini to further diversify them. As a result of the above diversification process, we constructed a number of instructions equivalent to approximately 2% of its total data volume for each task. In other words, each instruction appears around 50 times in the instruction-tuning dataset.

C Comparison of Rationales Generated by Teacher Models

As shown in Figure 3, 9, and 10, the rationales generated using our method exhibit distinct advantages in terms of accuracy, completeness, and logicality.

The advantage in accuracy is mainly reflected in Figure 3. In Figure 3, o3-mini completely misunderstands the chemical reaction that occurs between the given molecules. This might result from its incorrect identification of the reagents and the structure of the complex reactants (these errors are also reflected in the rationales). When given the correct answer, o3-mini still mistakenly identified

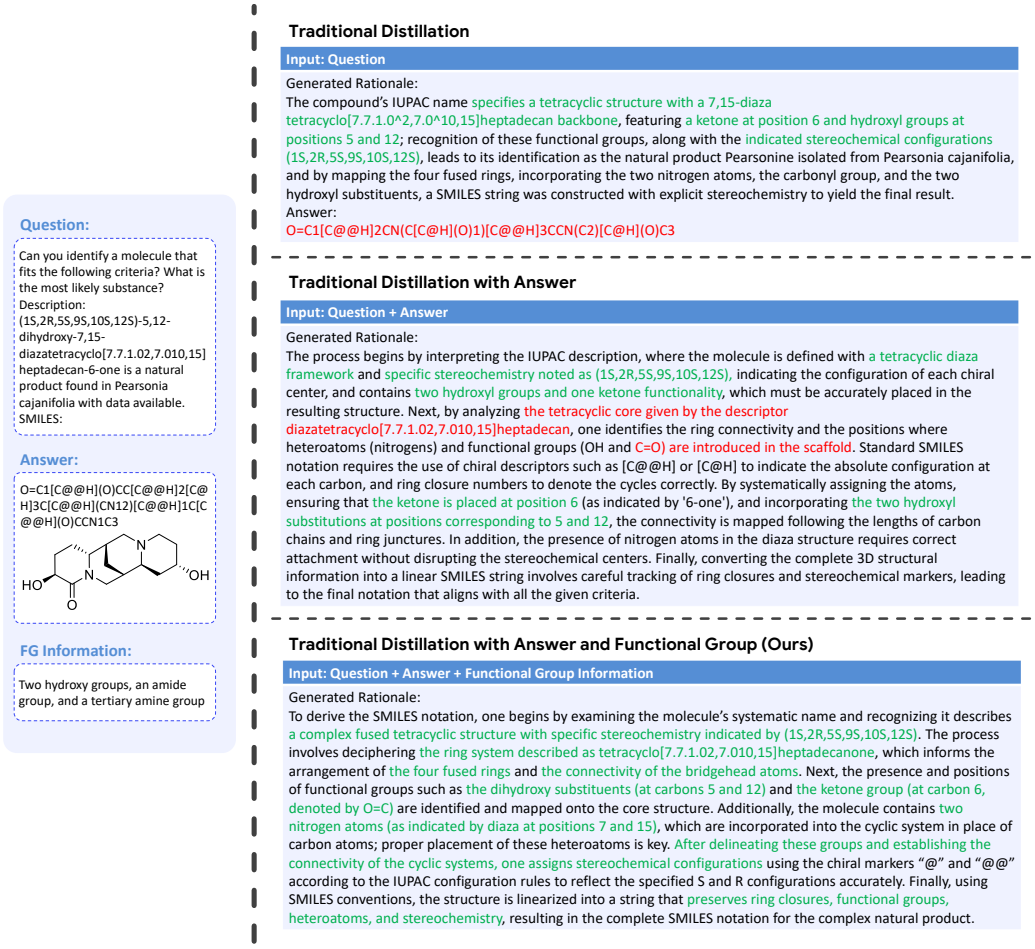

Figure 9: Comparison of rationales generated by o3-mini with and without additional input information. We mark the correct analyses in the rationale as green, while the wrong ones as red.

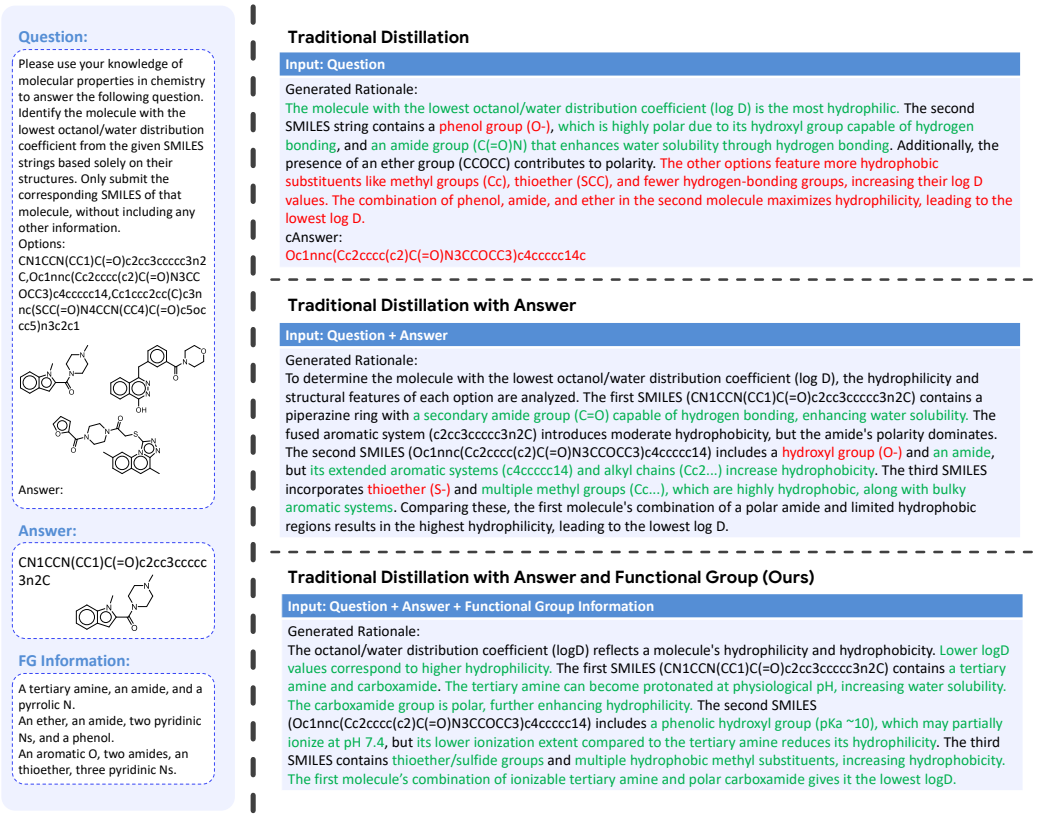

Figure 10: Comparison of rationales generated by DeepSeek-R1 with and without additional input information. We mark the correct analyses in the rationale as green, while the wrong ones as red.

chloro-ketone as acyl chloride and consistently adhered to this error throughout the reasoning process, resulting in a series of related structural inaccuracies. On the contrary, when the functional group information is provided, o3-mini manages to generate a near-perfect rationale with zero error.

The advantage in completeness is mainly reflected in Figure 9. In Figure 9, given only the question, DeepSeek-R1 only generates a brief analysis on the second option while dismissing the other three options with a single sentence in total. This overly simple analysis leads to a wrong prediction. With the help of the ground truth answer, the generated rationale analyzes all options individually. However, due to its lack of chemical knowledge, the analysis still exhibits errors in functional group recognition or overlooks key influencing factors. After enhancing chemical knowledge with the functional group information, DeepSeek-R1 finally manages to generate a more comprehensive analysis with few errors.

The advantage in logicality is mainly reflected in Figure 10. In Figure 10, with only the question, o3-mini can hardly generate any useful rational. The rational merely repeats the IUPAC components mentioned in the question before rushing to a highly inaccurate conclusion without substantive analysis. When given the ground truth answer, o3-mini can construct a reasonably good rationale with minimal factual error. However, the rationale still contains non-negligible issues in terms of logical coherence. A sound reasoning process should follow the approach exemplified by the reasoning chain generated by o3-mini using our method: analyzing in the order of molecular skeleton, functional groups, heteroatoms, and chiral centers. This sequence reflects a step-by-step refinement from the fundamental molecular structure to more intricate structural details. However, with only the question and answer, the generated rationale mixes these analytical steps and lacks critical details, such as the precise position of the nitrogen atom, resulting in a disorganized and incomplete reasoning process.

D Details of Reinforcement Learning

We use the DAPO (Yu et al., 2025) algorithm for reinforcement learning. For each training sample, we sample 8 different rollouts during training. The learning rate is set to 5e-7, and the batch sizes for rollouts and training are set to 512 and 128, respectively. As for the reward system, we follow the method recommended by DeepSeek-R1 (Guo et al., 2025), where the reward system consists of format rewards and accuracy rewards. The format rewards evaluate whether a response strictly follows the reasoning format, and the accuracy rewards evaluate whether a response is correct. Specifically, considering the redundancy of the casual SMILES notations (one molecule could correspond to multiple SMILES), we first canonicalize all the SMILES in the response before calculating the accuracy rewards.

E The Analysis of ChemDFM-R's Rationale

In Figure 11, ChemDFM-R is asked to pick a correct product for the given reaction. Instead of wasting time (tokens) on analyzing the SMILES in great detail, which DeepSeek-R1 always does, ChemDFM-R1 goes directly into the key point of this question: the functional groups present in the reactants and the potential reactions between them. Specifically, ChemDFM-R successfully identifies the key functional group, the carbamate ester group. By recalling that the carbamate ester group is typically used to protect amino groups, ChemDFM-R infers that the reaction taking place is likely a deprotection reaction. Then, ChemDFM-R confirms its assumption by examining the provided reagents. Finally, ChemDFM-R predicts the feature of the possible product and picks the option that matches it. This example demonstrates the precision of ChemDFM-R in finding the key point of chemical questions, and the effectiveness and efficiency of ChemDFM-R's rationales. Moreover, it is also worth noticing that, instead of using the "elimination-shortcut" which is commonly adopted by other cutting-edge reasoning LLMs, ChemDFM-R directly reasoned out the reaction mechanism and the features of the correct answer, thereby selecting the correct option.

As illustrated in Figure 12, when asked to describe a molecule given by SMILES, ChemDFM-R first analyzes the functional groups present in the molecule, such as the alkene group, the phosphate mono-ester group, and the pyrrolic N group. Then, ChemDFM-R successfully correlates the composition and connectivity of these functional groups with metabolic pathways and further manages to identify the molecule as a coenzyme A derivative. After that, it recognizes the deprotonated thiolester linkage

Question: Given a question and four options, please select the right answer. Your answer should be "A", "B", "C" or "D". Please directly give the answer without any explanation.
Given the reactants and reagents (in SMILES format) which are split by "." as follows:
CC(C)(C)OC(=O)NCCc1ccc(OCCC23CC4CC(CC(C4)C2)C3)cc1.CO.Cl
Which of the following candidate SMILES represents the correct product of this reaction?

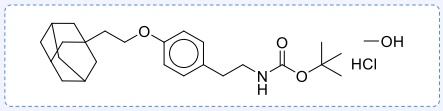

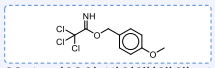

A. COc1ccc(COC(=N)C(Cl)(Cl)Cl)cc1

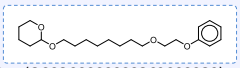

B. c1ccc(OCCOCCCCCCCCCOC2CCCCO2)cc1

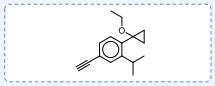

C. C#Cc1ccc(C2(OCC)CC2)c(C(C)C)c1

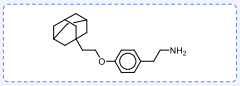

D. NCCc1ccc(OCCC23CC4CC(CC(C4)C2)C3)cc1

<think>
To approach the problem, one first confirms that the starting material **incorporates a carbamate ester group** (defined as an ester of carbonic acid that links to an –NH- fragment, which is often used **for protecting amino groups during synthesis**) and then considers that converting this functional group into a primary amine requires **a deprotection step**. This analysis involves recognizing that such transformations typically occur via **acid-catalyzed mechanisms**, where the reagents provided (including a molecule containing CO and Cl, which can function as a source of activating agents like an HCl, a common reagent for removing carbamate protecting groups) promote **the cleavage of the tert-butyl protecting group, leading to the formation of the free amine**. By examining the set of options supplied, only the selection whose structure contains the primary amine functionality, identified by an -NH2 attached directly to an aromatic ring substituted with an appropriate side chain (which matches the context provided in the reagent transformations), is consistent with this deprotection process. This methodical structural evaluation, considering both the reaction mechanism and the changes between the protecting group and the final product, leads to the selection of the correct molecule that exhibits the primary amine substitution pattern under the reaction conditions.
</think>
<answer>
D
</answer>

Figure 11: An example of the responses generated by ChemDFM-R on the reaction prediction task.

Question: You are an expert chemist. Given the molecule SMILES, your task is to provide the detailed description of the molecule using your experienced chemical knowledge.
Please strictly follow the format, no other information can be provided.

The Molecule SMILES is as follows:
CCCCCC/C=C/C(=O)SCCNC(=O)CCNC(=O)[C@H](O)C(C)(C)COP(=O)(O)OP(=O)(O)OC[C@H]1O[C@@H](N2C=NC3=C(N)N=CN=C32)[C@H](O)[C@@H]1OP(=O)(O)O

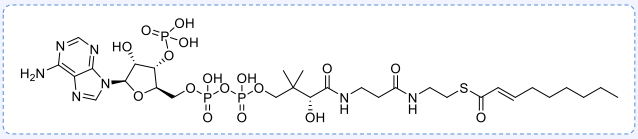

<think>
To derive the molecular description, one first examines the SMILES notation to identify the structural components such as the **alkene, hydroxy, ether, anhydride, primary amine, carboxamide, thiolester, and phosphate mono-ester groups**, as well as the aromatic heteroatoms like **pyrrolic N and pyridinic N**. Recognizing these functional groups and their connectivity, one then **correlates the structure with known biochemical molecules, particularly those involved in metabolic pathways**. By noting **the presence of a coenzyme A moiety and a deprotonated thiolester linkage, which are characteristic of acyl-CoA derivatives**, one can infer that the molecule is an acyl-CoA compound. This structural analysis, combined with knowledge of metabolic roles in organisms such as Escherichia coli and mouse, leads to the conclusion that **the molecule is a metabolite with a specific acyl group attached to coenzyme A**.
</think>
<answer>
The molecule is a medium-chain fatty acyl-CoA that results from the formal condensation of the thiol group of coenzyme A with the carboxy group of trans-2-nonenioic acid. It is a trans-2-enoyl-CoA, a medium-chain fatty acyl-CoA and a monounsaturated fatty acyl-CoA. It is a conjugate acid of a trans-2-nonenoyl-CoA(4-).
</answer>

Figure 12: The overview of the training pipeline of ChemDFM-R on the molecule captioning task.

Question: Please give the IUPAC name of the molecule given by SMILES: Cc1ccc(C(C)NC(=O)CCCN(c2cccc(Cl)c2)S(C)(=O)=O)c(C)c1.

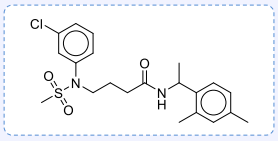

<think>
To derive the IUPAC name, one first examines the SMILES notation to identify the molecular structure, noting the presence of **an aromatic ring substituted with methyl groups, a secondary amine linkage, and a sulfonamide group attached to a benzene ring bearing a chloro substituent**. The next step involves **determining the connectivity and substituent positions on the aromatic system, ensuring that the substituents are numbered according to IUPAC rules to give the lowest possible locants**. The molecule is then divided into **its principal structural components, with one part being the substituted benzene ring and the other part being the acyl chain linked to the sulfonamide group. The acyl chain is further analyzed to determine its substituent pattern, including the N-substitution with the sulfonamide group**. By applying systematic nomenclature rules, including the priority of functional groups and the use of prefixes and suffixes to denote substituents and connectivity, the complete IUPAC name is constructed. This process integrates the identification of functional groups, the determination of substituent positions, and the systematic assembly of the name according to IUPAC guidelines.
</think>
<answer>
4-(3-chloro-N-methylsulfonylanilino)-N-[1-(2,4-dimethylphenyl)ethyl]butanamide
</answer>

Figure 13: The overview of the training pipeline of ChemDFM-R on the SMILES to IUPAC task.

in the molecule and further narrows down the molecule to an acyl-CoA derivative. Finally, ChemDFM-R gives a relatively comprehensive description of the molecule. ChemDFM-R even provides the potential role of this molecule in metabolic processes in its rationale, further demonstrating its strong reasoning ability as well as the value of the rationale as a complement to the final answer.

Figure 13 showcases an example response of ChemDFM-R when asked to generate the IUPAC name of the given molecule. The IUPAC name is the standard name for a molecule, assigned according to the rules established by the International Union of Pure and Applied Chemistry (IUPAC). It can effectively reflect the functional groups present in the molecule and their connectivity. Therefore, ChemDFM-R starts its reasoning with a comprehensive analysis of the functional groups of the given molecule. Then, it emphasizes the importance of correctly labeling the atoms, which is precisely an area where large language models are particularly prone to errors. After this, ChemDFM-R follows the rule of IUPAC naming and divides the molecule into its principal structural components. It also specifically points out the N-substitution with the sulfonamide group. Finally, a complicated and correct IUPAC name is predicted by ChemDFM-R.

F Detail Results of Benchmark Evaluation

F.1 ChemEval

We consider the L1 and L2 level tasks in ChemEval as text-centric tasks, the L3 level tasks as molecule-centric tasks, and the L4 level tasks as reaction-centric tasks. Moreover, there are tasks that we can not achieve a feasible grading in ChemEval. We temporarily skip these tasks. The raw results are demonstrated in Table 5.

As illustrated in Table 5, ChemDFM-R manages to achieve competitive performance in the text-centric tasks compared with the cutting-edge LLMs, while achieving SOTA performance across all the molecule-centric tasks and a large portion of the reaction-centric tasks. A detailed analysis of the task characteristics reveals that ChemDFM-R tends to perform less effectively on tasks involving numerical prediction, which will be a key focus of our future optimization efforts.

Tasks	Metric	MolInst	ChemLLM -20B-DPO	ChemDFM -13B-v1.0	ChemDFM -8B-v1.5	GPT-4o	Qwen3-14B (no think)	DeekSeek -R1	Qwen3-14B (think)	o4-mini	ChemDFM-R
Text-Centric Tasks											
MCTask	Acc	0.40	0.35	0.50	0.00	0.75	0.75	**0.90**	0.80	0.65	0.65
FBTask	Acc	0.00	0.00	**0.05**	0.00	0.00	0.00	0.00	0.00	0.00	0.00
TFTask	Acc	0.55	0.75	0.70	0.05	0.80	0.85	**0.95**	0.80	0.85	0.85
SATask	BLEU	0.01	**0.17**	0.12	0.11	0.15	0.09	0.04	0.07	0.10	0.13
CNER	F1	0.00	0.44	0.59	0.23	0.67	0.61	**0.70**	0.67	0.57	0.62
CERC	F1	0.05	0.00	0.12	0.00	0.20	0.24	**0.28**	0.20	0.26	0.26
AddE	F1	0.34	0.59	0.47	0.05	0.70	0.65	0.71	0.65	0.68	**0.72**
SolvE	F1	0.58	0.70	**0.83**	0.25	0.75	0.73	0.79	0.54	0.72	0.73
TempE	F1	0.70	0.75	0.20	0.25	0.75	**0.95**	**0.95**	0.90	**0.95**	**0.95**
TimeE	F1	**0.95**	**0.95**	0.40	**0.95**	**0.95**	**0.95**	**0.95**	**0.95**	**0.95**	**0.95**
CharME	F1	0.21	0.47	0.26	0.49	**0.79**	0.74	0.71	0.61	0.76	0.49
CatTE	F1	0.80	0.90	0.55	0.30	0.95	0.85	**1.00**	0.85	0.90	0.75
YieldE	F1	0.00	0.55	0.20	0.30	0.80	0.75	0.75	**0.95**	0.75	0.60
AbsGen	BLEU	0.56	0.46	0.54	0.04	0.67	**0.70**	0.62	0.65	0.67	0.69
OLGen	BLEU	0.19	0.12	0.22	0.02	0.14	**0.24**	0.10	0.18	0.13	0.15
TopC	Acc	0.40	0.50	0.40	0.20	0.50	0.40	**0.55**	0.50	0.50	0.50
ReactTR	F1	0.20	0.13	0.15	0.05	**0.35**	0.30	0.25	0.30	0.20	0.30
Molecule-Centric Tasks											
MolNG	BLEU	0.04	0.57	0.76	0.35	0.60	0.43	0.10	0.42	0.69	**0.84**
IUPAC2MF	EM	0.00	0.00	0.25	0.00	0.40	0.00	0.05	0.00	0.60	**0.75**
SMILES2MF	EM	0.00	0.00	0.45	0.00	0.10	0.05	0.00	0.00	0.55	**0.85**
IUPAC2SMILES	EM	0.00	0.00	0.10	0.00	0.00	0.00	0.05	0.00	0.15	**0.55**
SMILES2IUPAC	EM	0.00	0.00	0.00	0.05	0.00	0.00	0.00	0.00	0.00	**0.35**
S2S	EM	0.00	0.00	0.00	0.00	0.00	0.00	0.00	0.00	0.00	0.00
MolPC	Acc	0.50	0.53	0.61	0.09	0.64	0.54	0.57	0.59	0.66	**0.73**
Mol2PC	BLEU	0.30	0.36	0.39	0.19	0.37	0.41	0.30	0.38	0.34	**0.57**
Reaction-Centric Tasks											
SubRec	Acc	0.00	0.03	0.08	0.02	0.08	0.00	0.05	0.00	0.18	**0.25**
LRec	Acc	0.00	0.00	0.20	0.00	0.10	0.05	0.10	0.35	0.00	**0.45**
RRec	Acc	0.00	0.00	0.19	0.00	0.10	0.15	0.05	0.25	0.30	**0.35**
SolvRec	Acc	0.00	0.00	0.05	0.00	0.35	0.02	0.25	0.35	0.30	**0.40**
CatRec	Acc	0.00	0.00	0.00	0.00	0.00	0.00	0.00	0.00	0.00	0.00
TempRec	RMSE ↓	0.77	0.27	0.71	0.22	0.22	0.23	**0.18**	0.35	0.22	0.30
TimeRec	RMSE ↓	0.20	0.19	0.18	0.09	**0.07**	0.08	0.10	0.11	0.10	0.15
PPre	Acc	0.00	0.00	0.03	0.05	0.10	0.00	0.18	0.06	0.35	**0.60**
YPred	Acc	0.20	0.20	0.20	0.00	**0.55**	0.15	0.25	0.25	0.45	0.20
RatePred	Overlap	0.03	0.14	0.05	0.09	0.18	0.15	**0.31**	0.10	0.07	0.09
IMDer	Acc	0.00	0.00	**0.10**	0.00	0.05	0.00	0.05	0.00	0.05	0.00

Table 5: The detailed benchmark results of different models on ChemEval.

Turn1: What is oxygen evolution reaction (OER)? Please propose a reasonable mechanism of heterogeneous OER under acidic conditions.

<think>
To derive the answer, one starts by defining the oxygen evolution reaction (OER) as the electrochemical process that converts water into molecular oxygen, which is a critical step in water splitting. Recognizing that OER can occur under both acidic and basic conditions, the focus is on the mechanism under acidic conditions, where the reaction involves protons (H+) and water molecules. **The process is typically facilitated by a catalyst, often a transition metal oxide, which provides active sites for the reaction.** **The mechanism is then broken down into several steps: first, the adsorption of water molecules onto the catalyst surface, followed by the formation of an intermediate species such as an adsorbed hydroxyl group (OH–) or a water-derived species. Subsequent steps involve the transfer of protons and electrons, leading to the formation of an oxygen-oxygen bond, which is a key step in the reaction. Finally, the desorption of molecular oxygen (O2) from the catalyst completes the cycle.** This sequence of adsorption, intermediate formation, bond formation, and desorption is consistent with the known electrochemical steps in OER under acidic conditions, and it is supported by experimental observations and theoretical models.
</think>
<answer>
The oxygen evolution reaction (OER) is an electrochemical process that involves the conversion of water into molecular oxygen (O2) and protons (H+). In heterogeneous OER under acidic conditions, the reaction typically occurs on a solid catalyst surface. The mechanism can be described as follows:

1. **Water adsorption**: Water molecules (H2O) adsorb onto the catalyst surface.
2. **Proton transfer**: Protons (H+) are transferred from the adsorbed water molecules to the catalyst surface, forming hydroxyl (OH-) groups.
3. **Oxygen adsorption**: The hydroxyl groups further react to form adsorbed oxygen species (O*), which are intermediates in the reaction.
4. **Oxygen evolution**: The adsorbed oxygen species combine to form molecular oxygen (O2), which desorbs from the catalyst surface and enters the solution.

The overall reaction can be represented as:

2H2O → O2 + 4H+ + 4e-
</answer>

Turn2: Since you mentioned in your thinking that the formation of oxygen-oxygen bond is the key to the reaction, please give an intermediate that reflect the formation of oxygen-oxygen bond and improve the mechanism you provided.

<think>
To incorporate the formation of the oxygen-oxygen bond into the mechanism, one starts by recognizing that this bond formation is a critical step in the oxygen evolution reaction (OER). **The process involves the generation of an adsorbed oxygen species (O) on the catalyst surface, which then undergoes a transformation to form an intermediate that contains the oxygen-oxygen bond. This intermediate is typically represented as a peroxide-like species (OOH) or a superoxide-like species (O2–), depending on the specific reaction conditions and the electronic properties of the catalyst. The formation of this bond is facilitated by the transfer of protons and electrons, which are provided by the acidic environment and the catalyst, respectively. The stabilization of the intermediate is crucial for the subsequent steps, including the final desorption of molecular oxygen (O2) from the catalyst surface.** By integrating these specific intermediates and their roles in the mechanism, one can clearly illustrate how the oxygen-oxygen bond is formed and how it contributes to the overall OER process under acidic conditions.
</think>
<answer>
In the mechanism of the oxygen evolution reaction (OER) under acidic conditions, the formation of the oxygen-oxygen bond is a critical step. This bond formation occurs through the generation of an intermediate species that contains two oxygen atoms. The specific intermediate formed depends on the reaction conditions and the catalyst used.

One possible intermediate is the peroxide species (OOH), which is formed when two hydroxyl groups (OH-) undergo a coupling reaction. This coupling reaction involves the transfer of an electron and a proton, leading to the formation of the peroxide bond (O-O).

Another possible intermediate is the superoxide species (O2–), which is formed when an oxygen atom (O) undergoes a one-electron reduction. This reduction can occur through the transfer of an electron from the catalyst surface or from another oxygen species.

The formation of these intermediates is essential for the subsequent steps in the OER mechanism, including the final desorption of molecular oxygen (O2) from the catalyst surface. The stability and reactivity of these intermediates are influenced by factors such as the electronic properties of the catalyst and the reaction conditions (e.g., pH, temperature).
</answer>

Figure 14: An example of reliable human-AI collaboration using ChemDFM-R. We draw inspiration from this conversation from Li et al. (2025). This example illustrates a process of error detection and correction with the help of rationales.

F.2 SciKnowEval

We group the tasks in SciKnowEval based on their input and output. Specifically, the task is classified as a text-centric task if there is no SMILES appear in its input or output, as a reaction-centric task if there are reaction SMILES appear in its input or output, and as a molecule-centric task otherwise. Due to budget limit, we currently skip the tasks that require GPT-4o for grading. The raw results are demonstrated in Table 6.

As illustrated in Table 6, ChemDFM-R achieves competitive performance on SciKnowEval compared to cutting-edge LLMs. It is worth noting that ChemDFM-R's performance advantage is less pronounced on SciKnowEval than on ChemEval. This is primarily because most tasks in SciKnowEval are formulated as multiple-choice questions, which substantially reduce the burden on the model's comprehension and generation processes, allowing it to arrive at correct answers through "shortcuts" such as option comparison and elimination.

G More Examples of Reliable Human-AI Collaboration

Figure 14 illustrates a conversation starting from the same turn as that illustrated in the main text. In this conversation, we focus on fully understanding the mechanism of the oxygen evolution reaction (OER). Suppose, as a newbie, we are unable to determine the correctness of the answer. With the help of ChemDFM-R's rationale, we could easily discover that the key step of the reaction mentioned in the rationale, which is "the formation of an oxygen-oxygen bond", is absent in the answer. This could serve as a reminder that the answer could be incorrect, and drive us to further request the model to clarify this inconsistency. After this follow-up inquiry, the model provided a better answer.

Tasks	MolInst	ChemLLM -20B-DPO	ChemDFM -13B-v1.0	ChemDFM -8B-v1.5	GPT-4o	Qwen3-14B (no think)	DeekSeek -R1	Qwen3-14B (think)	o4-mini	ChemDFM-R
Text-Centric Tasks										
Chem LiterQA	0.75	0.79	0.78	0.80	0.86	0.84	0.86	0.84	**0.89**	0.80
React Mech Infer.	0.96	0.99	0.98	0.99	**1.00**	0.99	0.97	0.98	0.98	0.98
Comp Iden. and Prop.	0.94	0.97	0.95	0.97	**0.99**	0.98	0.96	**0.99**	**0.99**	0.98
Chem DU	0.95	0.98	0.97	0.97	**1.00**	0.99	0.99	0.99	0.99	0.98
Chem HV	0.83	0.89	0.86	0.88	**0.95**	0.94	0.93	0.92	0.93	0.92
Chem RI	0.93	0.96	0.95	0.96	**0.97**	**0.97**	0.95	0.96	0.96	**0.97**
Balancing Eq.	0.01	0.16	0.12	0.22	0.10	0.08	0.11	**0.73**	0.10	0.27
Chem Cal.	0.35	0.33	0.37	0.37	0.52	0.54	0.79	0.91	**0.92**	0.54
Mol Tox. Pred	0.54	0.54	0.44	0.45	0.37	0.52	**0.62**	0.51	0.55	0.44
Chem Safe Test	0.69	0.75	0.60	0.65	**0.85**	0.81	0.82	0.83	0.80	0.81
Molecule-Centric Tasks										
Mol Name Conv.	0.60	0.71	0.70	0.83	0.87	0.71	0.42	0.84	**0.96**	0.90
Mol Prop. Pred	0.32	0.34	0.38	**0.48**	0.44	0.38	0.41	0.42	**0.48**	0.45
Mol Cap.	0.14	0.21	0.23	0.22	0.14	0.09	0.13	0.10	0.14	**0.51**
Mol Weight Cal.	0.26	0.26	0.17	0.23	0.26	0.17	0.04	0.31	**0.63**	0.37
Mol Prop. Cal.	0.39	0.33	0.31	0.30	0.35	0.37	0.39	0.38	**0.45**	0.20
Mol Stru. Pred	0.33	0.31	0.35	0.26	0.46	0.31	0.07	0.37	**0.57**	0.34
Mol Gen.	0.64	0.53	0.84	**0.89**	0.61	0.39	0.69	0.44	0.75	0.83
Reaction-Centric Tasks										
Reaction Pred	0.39	0.93	0.92	0.96	0.48	0.91	0.82	0.94	**0.99**	**0.99**
Retrosynthesis	0.44	0.83	0.78	0.77	0.41	0.70	0.83	0.83	**0.95**	0.90

Table 6: The detailed benchmark results of different models on SciKnowEval.

Turn1: I have used m-CPBA to convert the carbon-carbon double bond within the [H][C@]12CC[C@@]3(CC[C@]1C)C(=O)C1=C[C@@]4(C)CC[C@@](C(C)C)[C@]4([H])C[C@]1([H])[C@]23C into an epoxide, and obtained chiral epoxy products with different ratios (d.r. = 5:1). Please propose possible reasons.

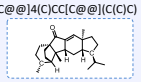

<think>
The reaction involves m-CPBA (meta-chloroperbenzoic acid) oxidizing a carbon–carbon double bond in a complex cyclic structure to form an epoxide. **m-CPBA acts as an electrophilic oxidizing agent, where the peracid's oxygen attacks the double bond, forming a cyclic transition state.** The stereochemical outcome is influenced by the complex cyclic framework's rigidity and steric factors. **The double bond's geometry and the spatial arrangement of substituents around the double bond determine which face of the alkene is more accessible to the electrophilic oxygen from m-CPBA.** The complex cyclic system imposes constraints that favor one diastereomeric pathway over another, leading to a 5:1 diastereomeric ratio. **The chiral centers in the complex cyclic structure further influence the transition state energies, with one pathway being thermodynamically favored due to reduced steric strain or optimal orbital overlap during the epoxidation process.**
</think>
<answer>
The complex cyclic framework of the molecule and the steric factors around the double bond lead to a preferential attack by the oxidant on one face of the double bond, resulting in a diastereomeric ratio of 5:1.
</answer>

Turn2: Please explain in detail how double bond's geometry and spatial arrangement of substituents around the double bond determine which face of the alkene is more accessible.

<think>
The spatial arrangement of substituents around the double bond in the complex cyclic structure creates steric hindrance, which influences the accessibility of the alkene face to the oxidizing agent**. The complex cyclic framework imposes rigidity, restricting the approach of m-CPBA to one face of the double bond. Substituents such as methyl group create steric bulk, favoring the less hindered transition state during epoxidation. Additionally, electronic factors, including the electron-donating or electron-withdrawing nature of substituents, further modulate the reactivity of the alkene face.** The combination of steric and electronic effects results in a preferential attack on the less congested face, leading to the observed diastereomeric ratio of 5:1 in the epoxide products.
</think>
<answer>
The complex cyclic structure imposes steric constraints that influence the accessibility of the double bond to the oxidizing agent. The arrangement of substituents around the double bond creates a situation where one face is more sterically accessible than the other, leading to a preference for the oxidizing agent to attack from that side, which is reflected in the diastereomeric ratio of the resulting epoxide products.
</answer>

Figure 15: An example of reliable human-AI collaboration using ChemDFM-R. We draw inspiration from this conversation from Yao et al. (2025). This example illustrates a process of information completion.

Figure 15 is a conversation about a reaction proposed in Yao et al. (2025). We first ask ChemDFM-R to explain the reason for the different ratios of the chiral epoxy products. Although the model's answer is relatively broad, ChemDFM-R thoroughly analyzes the influence factors in its rationale, including the bond's geometry and the spatial arrangement of substituents around the double bond, which is not included in the answer. With this information, we can further pursue the follow-up question and obtain an improved answer.